

# Optimizing Multiple Beam Patterns for 5G mmWave Phased Array Applications

Jafar Ramadhan Mohammed<sup>1\*</sup>

<sup>1</sup> Department of Communications Engineering, College of Electronics Engineering, Ninevah University, Right Coast, Jawsaq, Mosul 41002, Iraq

\* Corresponding author, e-mail: [jafar.mohammed@uoninevah.edu.iq](mailto:jafar.mohammed@uoninevah.edu.iq)

Received: 25 February 2023, Accepted: 05 May 2023, Published online: 08 June 2023

## Abstract

In this paper, a new technique for shaping multiple beam patterns antenna arrays for 5G and beyond wireless massive MIMO communication systems is introduced. The technique aims to concentrate the radio energy in specific coverage areas with a desired shape by optimizing the excitation amplitudes and phases of the array elements. To assess the proposed technique, both genetic algorithm and particle swarm optimization are utilized to optimize the excitation amplitudes and phases of the array elements such that the required number of the beams, their shapes, their directions, their power magnitudes, and the desired sidelobe pattern can be achieved. Simulation results fully confirm the effectiveness of the proposed technique in generating optimized shaped patterns that can be suitably used for distributing the radiation powers over the coverage areas in the mobile communication base stations.

## Keywords

antenna arrays, 5G wireless communications and beyond, array pattern optimization, shaped multiple beams

## 1 Introduction

For high-precision communications and improved spectral efficiency, the radiated power by a transmitted antenna array should be efficiently and precisely distributed according to the required coverage area(s). Applications include energy management in the wireless communications (where closer targets to the base stations can be illuminated with a lower gain beam), satellites (specifically, satellite-borne array antenna where its pattern shape should be conformed precisely to the shape of the required coverage area on the earth [1]), optical communications (specifically, optical phased arrays to steer multiple laser beams [2]), and modern radar systems. The key element in these applications is the antenna array, whose main design parameters are geometrical layout of the array elements, the inter-element spacing, the excitation amplitudes and phases of the individual elements, and finally the elemental beam pattern which they can be separately or jointly controlled to generate a single or multiple beams in the desired directions and place nulls in the interference directions.

In most of the published works in the literature, the antenna arrays were used to generate single beams with highly focused directive power [3–6]. However, it is also possible to produce multiple beams from the same array

aperture using multiple feeder networks for example see [7, 8]. Other methods used switched beam approaches [9] to realize multiple beams. Some specific shapes like flat-top, cosecant-squared, sum, or any other array patterns can be obtained by modifying the corresponding excitation amplitudes and phases of the array elements [1, 10, 11]. It is found, in general, that the optimization algorithms are more suitable than the analytical methods for shaping the multiple beam patterns. However, the convergence speeds of such optimizers depend on the number of design variables such as array geometry and excitation weights. Thus, many partially common excitation approaches have been proposed to reduce the number of the design variables and simplify the array feeding network [12–15].

In this paper, we introduce an efficient optimization technique based on the pre-specified mask constraints to generate multiple simultaneous and reconfigurable shaped beam patterns. A suitable cost function is applied to perform the desired constraint masks on the array radiation patterns. Two optimization algorithm tools such as genetic algorithm and the particle swarm optimization are used to verify such constraint masks. The number of the main beams, their shapes, their directions, their relative power

magnitudes, and the desired sidelobe levels can be obtained according to the given mask using a single array aperture irrespective of its size and geometry. Further, the method is also able to place nulls in assigned directions in conjunction with the generations of required multiple beams. Furthermore, the technique is quite simple and fast.

**2 The proposed technique**

The radiation pattern of a linear antenna array consists of  $N$  elements distributed along the  $x$  axis with inter-element spacing,  $d$ , can be written as

$$AP_{\text{single beam}}(\theta) = \sum_{n=1}^N \underbrace{EP_n(\theta)}_{\text{Element Pattern}} \underbrace{w_n e^{j(n-1)\frac{2\pi}{\lambda}d\sin(\theta)}}_{\text{Array Factor}}, \quad (1)$$

where  $w_n = a_n e^{j\phi_n}$  is the excitation amplitude and phase of the  $n^{\text{th}}$  element respectively,  $\lambda$  denotes the wavelength, and  $\theta$  is the observation angle normal to the array. For the case of non-isotropic elements, the element pattern may be chosen as  $EP_n(\theta) = \cos(\theta)$ , while for isotropic elements it may be simply set to  $EP_n(\theta) = 1$ .

To generate multiple simultaneous beams equal to  $B$  toward the required directions with different tower levels,  $P_1(\theta_1), P_2(\theta_2), \dots P_B(\theta_B)$ , the array pattern of Eq. (1) can be rewritten as

$$AP_{\text{multibeam}}(\theta) = \sum_{n=1}^N w_n \left[ \sum_{b=1}^B P_b e^{-j(n-1)\frac{2\pi}{\lambda}d\sin(\theta_b)} \right] e^{j(n-1)\frac{2\pi}{\lambda}d\sin(\theta)}, \quad (2)$$

where  $B$  simultaneous beams are placed at the directions  $\theta_1, \theta_2, \dots \theta_B$ , the power level of each beam is represented by  $P_1(\theta_1), P_2(\theta_2), \dots P_B(\theta_B)$ . The half beam widths are assumed to be  $\Delta\theta_1, \Delta\theta_2, \dots \Delta\theta_B$ , respectively. Moreover, it is assumed there are a number of  $Z$  nulls placed at the interfering directions  $\theta_1, \theta_2, \dots \theta_Z$ , and the sidelobe level is as low as possible in all other directions. To satisfy these constraints, we consider the following mask function:

$$\text{Mask}(\theta) = \begin{cases} P_1(\theta_1), & -\Delta\theta_1 \leq \theta_1 \leq \Delta\theta_1 \\ \vdots & \\ P_B(\theta_B), & -\Delta\theta_B \leq \theta_B \leq \Delta\theta_B \\ \text{SLL}_{\text{Desired}}, & -\Delta\theta_{\text{SLL}} \leq \theta \leq \Delta\theta_{\text{SLL}} \\ \text{Null}_{\text{depth}}^1, & \theta = \theta_1 \\ \vdots & \\ \text{Null}_{\text{depth}}^Z, & \theta = \theta_Z \end{cases} \quad (3)$$

In order to get best match between the array pattern in Eq. (2) and the desired mask in Eq. (3), they are both vertically and equally divided into  $M$  different horizontal sample angles. For each horizontal angle, the difference (error) between them is determined by computing

the difference between the obtained power level and the desired mask limit as follows:

$$e_m = AP(\theta_m) - \text{Mask}(\theta_m), \quad m = 1, 2, \dots M. \quad (4)$$

A least mean square (LMS) minimization criterion is used to find the undesired error in the beam shape region as

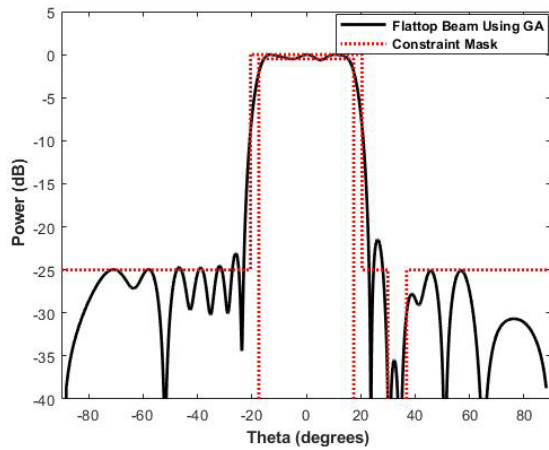
$$\text{Error} = \sqrt{\frac{1}{M} \sum_{m=1}^M |e_m|^2}. \quad (5)$$

Equation (5) represents the fitness value, and it should be as small as possible to get the best results. To assess the effectiveness of the proposed technique, a single flat-top beam pattern with half beam width equal to  $\Delta\theta = 20^\circ$ , one desired wide null centered at  $\text{Null}_{\text{Desired}} = 34^\circ$ ,  $\text{SLL}_{\text{Desired}} = -25$  dB, and the total sample points  $M = 512$  is generated by using both GA and PSO as shown in Figs. 1 and 2 respectively. The variations of the fitness function of these two optimization algorithms are shown in Fig. 3. It can be seen that the result of the GA is better than that of the PSO especially in the main lobe region where the maximal ripple in the flattop beam region between  $-20^\circ \leq \Delta\theta \leq 20^\circ$  is less than  $-0.5$  dB and the obtained sidelobe level is below  $-20$  dB. More important, the GA is capable to exactly fit all the mask constraints, while the PSO fails. In addition, the execution time of the GA and the PSO to obtain such results are 0.052962 minutes and 0.033701 minutes respectively.

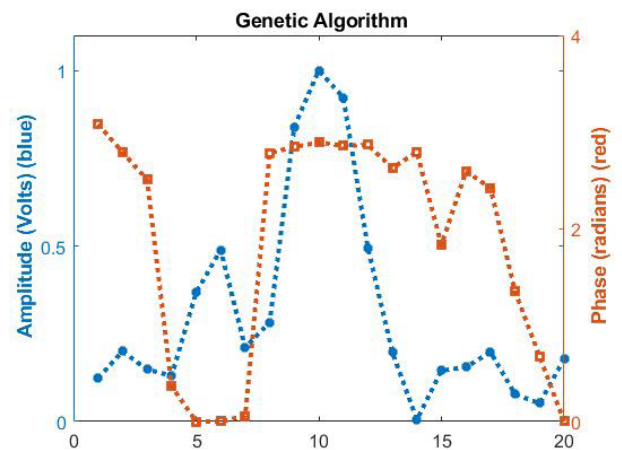
Another practical application of the proposed technique is in the mobile base station where the radiation pattern of its designed antenna array can be suitably shaped to fit the service area. The interference between mobile cells can be significantly reduced by concentrating the radio energy inside the covered cell while preventing it to reach other cells that reuse the same frequency. A collinear array composed of 10 elements distributed along  $z$ -axis and spaced by  $d = 0.5\lambda$  is considered in this scenario. According to the Friis transmission equation, the transmit antenna gain,  $G_T$ , can be represent by Eq. (6) [6]:

$$G_T(\theta) = \frac{P_R}{P_T G_R(\theta)} \left( \frac{2\pi h}{\lambda} \right)^2 \frac{1}{\cos^2 \theta}, \quad (6)$$

where  $P_R$  is the received power by a mobile,  $P_T$  is the transmitted power by the base station,  $G_R(\theta)$  is the received antenna gain of the mobile user which may be considered constant over  $\theta$ , where  $\theta$  is the elevation angle,  $h$  is the height of the transmit antenna, and  $\lambda$  is the wavelength. Note that the radiation pattern gain of the transmitted antenna array is distributed like secant-squared over the

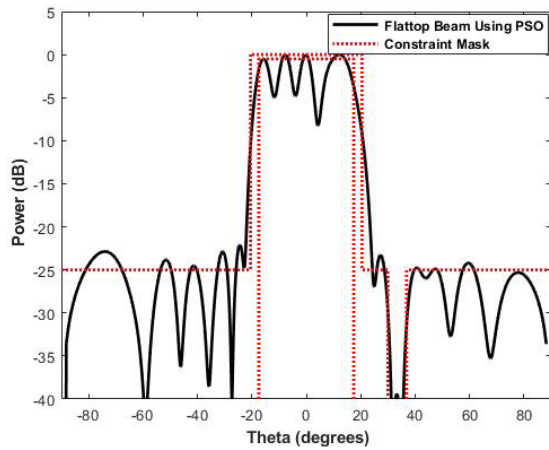


(a)

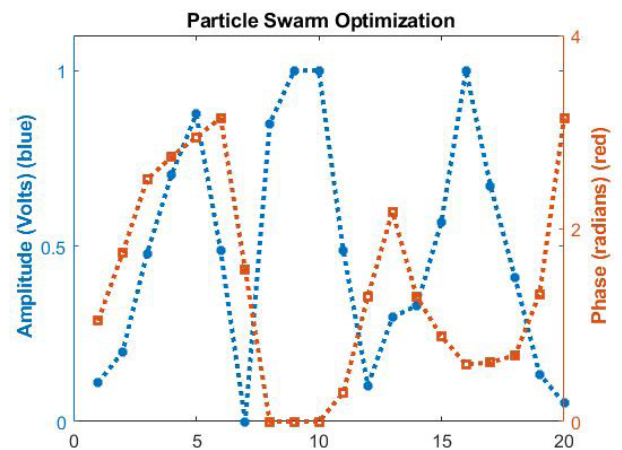


(b)

Fig. 1 Shaped pattern obtained using GA (a) and its corresponding amplitude and phase excitations (b)



(a)



(b)

Fig. 2 Shaped pattern obtained using PSO (a) and its corresponding amplitude and phase excitations (b)

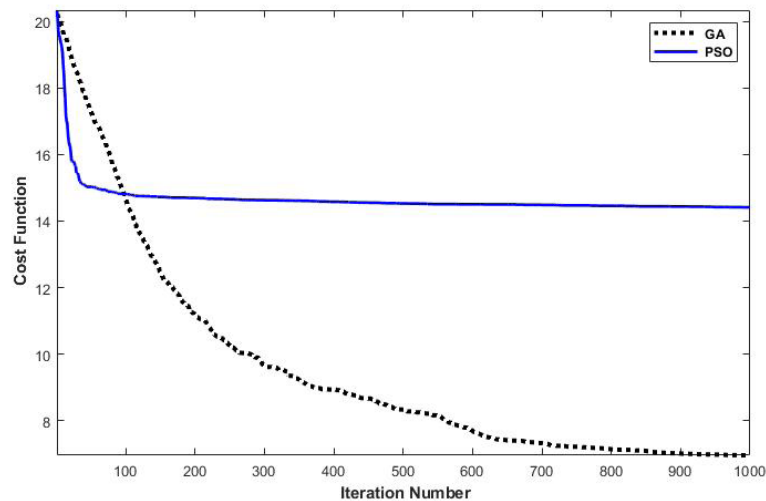


Fig. 3 Cost function variations for GA and PSO for the results that shown in Fig. 1 and Fig. 2

required service area  $\theta_2 \leq \theta \leq 180^\circ$  and it should be minimum outside the service area within the angular range  $0^\circ \leq \theta \leq \theta_1$  to reduce the interference (see Fig. 4 (a)).

Here,  $\theta_1 = 95^\circ$ ,  $\theta_2 = 105^\circ$ , and the  $SLL_{Desired} = -20$  dB within the angular range  $0^\circ \leq \theta \leq 95^\circ$ . The result is generated by optimizing the excitation amplitudes and phases

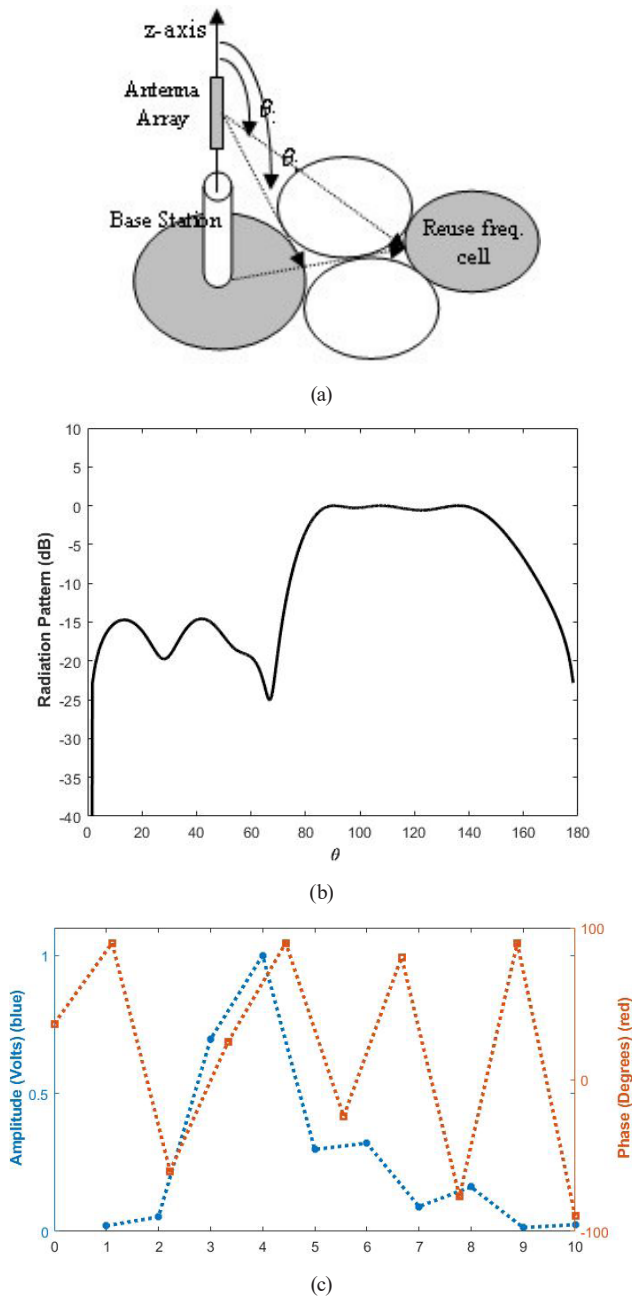


Fig. 4 (a) Base station model, and (b) secant-squared array pattern, (c) amplitudes and phases of pattern in (b)

of the array elements using GA as shown in Fig. 4 (b). The optimized amplitude and phase excitations of the base station antenna array are shown in Fig. 4 (c). It can be seen from Fig. 4 (b) that the obtained SLL is about  $-16$  dB within the angular range  $0^\circ \leq \theta \leq 90^\circ$ , while the main beam width covers the angular range  $105^\circ \leq \theta \leq 180^\circ$ .

### 3 Simulation results

In the following examples, a single linear antenna array composed of 20 elements spaced by  $d = 0.5\lambda$  is considered to generate the required shaped patterns. The used

specifications of the GA were set as follows; an initial population size of 50, number of iterations is set to 1000, selection is roulette, number of crossovers is 2, mutation probability is 0.04, and mating pool is chosen to be 4. The minimum and the maximum values of the excitation amplitudes and phases are bounded between  $0 \sim 1$  and  $-90^\circ \sim 90^\circ$  respectively. Note that the proposed method is also capable to control the dynamic range ratio  $DRR = |a_{\max}|/|a_{\min}|$  of the antenna array excitations by choosing the bounded values of the amplitude excitations. For example, if the minimum amplitude bound is chosen to start from  $a_{\min} = 0.2$  and  $a_{\max} = 1$ , then the  $DRR = 5$ . Note that this parameter is very important in the practical implementation of the array feeding network.

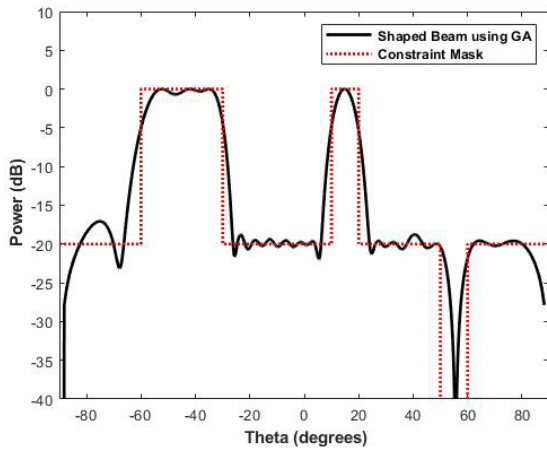
The first example optimizes the excitation amplitudes and phases of the antenna array to impose two specific main beams  $B = 2$  and a single wide null using the fitness function of Eq. (3) where the peak power in each beam is set to  $P_1(\theta_1) = P_2(\theta_2) = 0$  dB, the half width of each beam is  $\Delta\theta_1 = 15^\circ$ ,  $\Delta\theta_2 = 5^\circ$ , the  $SLL_{\text{Desired}} = -20$  dB, the depth and the width of the null is  $Null_{\text{depth}}^1 = -60$  dB and  $10^\circ$  (centered at  $55^\circ$ ) respectively. The optimized pattern is obtained using the GA as shown in Fig. 5. Fig. 5 also shows the optimized amplitude and phase excitations of the array elements. From Fig. 5, it can be seen that the required two beams and a single wide null were exactly placed according to the specified constraint mask. On the other hand, the PSO was unable to generate an optimized pattern according to such constraints, thus, the results of PSO were not shown here.

As a second example, a shaped pattern with  $B = 3$  peaks, half beam widths equal to  $\Delta\theta_1 = \Delta\theta_2 = \Delta\theta_3 = 10^\circ$  and  $SLL_{\text{Desired}} = -20$  dB is synthesized using the same number of array elements as in the previous example. The results of the GA are shown in Fig. 6. Again, the PSO was unable to satisfy such constraints.

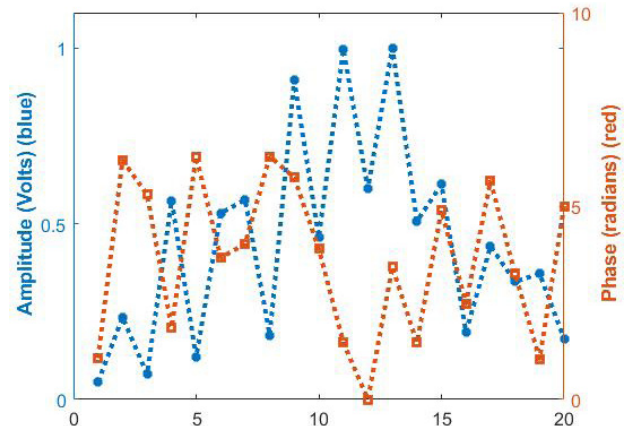
As a third example, a wide shaped beam with a width equal to  $60^\circ$  and  $SLL_{\text{Desired}} = -20$  dB is synthesized using the same parameters as in pervious. The results are shown in Fig. 7. Good agreement between the obtained beam using GA and the desired constraint mask is also observed. These results fully confirm the effectiveness and powerful of the GA in conjunction with the described constraint mask for generating specific pattern shapes according to the demanded coverage regions.

Finally, a shaped pattern with  $B = 4$  peaks and  $SLL_{\text{Desired}} = -30$  dB is designed. The power levels of the first and third peaks are made lower than the other two



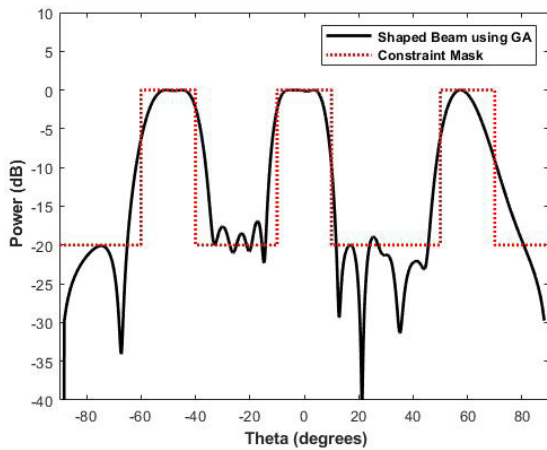


(a)

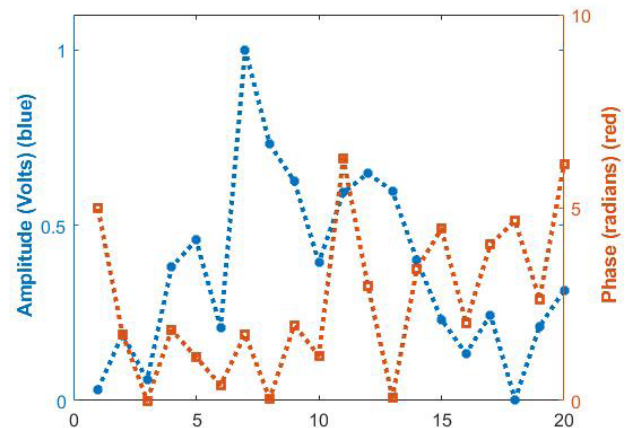


(b)

**Fig. 5** Obtained shaped pattern (a) and its corresponding amplitude and phase excitations (b) for  $B = 2$  peaks,  $Z = 1$  null, and  $SLL_{desired} = -20$  dB

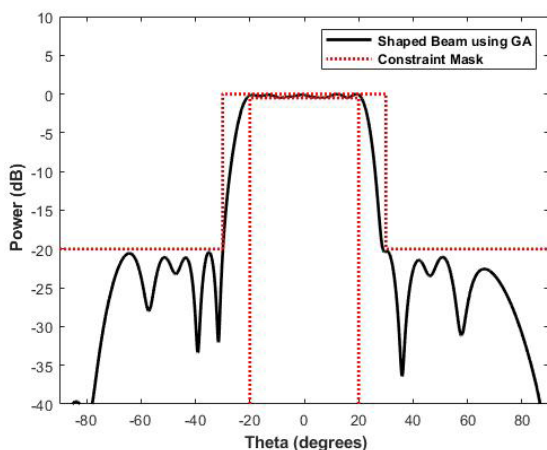


(a)

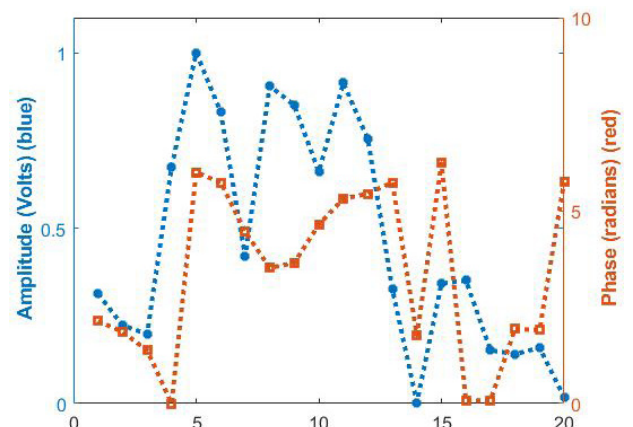


(b)

**Fig. 6** Obtained shaped pattern (a) and its corresponding amplitude and phase excitations (b) for  $B = 3$  peaks, and  $SLL_{desired} = -20$  dB



(a)



(b)

**Fig. 7** Obtained shaped pattern (a) and its corresponding amplitude and phase excitations (b) for a single wide beam and  $SLL_{desired} = -20$  dB

peaks by  $-6$  dB. The power levels of these four peaks were  $-6$  dB,  $0$ ,  $-6$  dB, and  $0$ . The results of the GA are shown in Fig. 8. As can be seen that the entire required multiple peaks are obtained.

#### 4 Conclusions

An effective synthesis technique for modern antenna arrays is proposed to generate multiple simultaneous and reconfigurable beams according to the demanded coverage

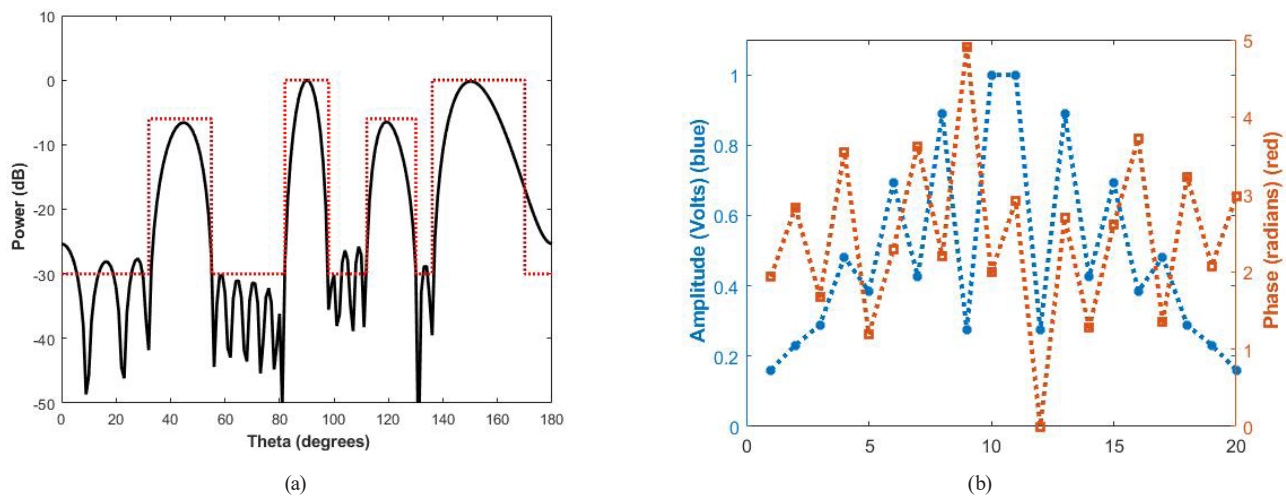


Fig. 8 Obtained shaped pattern (a) and its corresponding amplitude and phase excitations (b) for  $B = 4$  peaks, different power levels and  $SLL_{\text{desired}} = -30$  dB

regions. The cost function was formulated according to the specific constraint mask that best describes the desired pattern shapes and an optimization algorithm such as GA or PSO were used to generate the required array patterns by optimizing the excitation amplitudes and phases.

Results verified the effectiveness, simplicity, and versatility of the proposed technique. It provides a high

degree of control over the pattern's shape, and a flexible way in choosing the array excitations. Further, the technique is relatively fast. Moreover, this technique can be further extended to the planar arrays in geostationary satellite applications to generate shaped patterns to cover the map land of any country or continent for better power management.

## References

- [1] Salas-Sánchez, A. Á., López-Álvarez, C., Rodríguez-González, J. A., López-Martín, M. E., Ares-Pena, F. J. "An Improved Pattern Synthesis Iterative Method in Planar Arrays for Obtaining Efficient Footprints with Arbitrary Boundaries", *Sensors*, 21(7), 2358, 2021. <https://doi.org/10.3390/s21072358>
- [2] Wu, L., Wang, X., He, X., Huang, Z., Huang, X., Xiong, C. "Arbitrary multiple beam forming by two cascaded liquid crystal optical phased arrays", *Optics Express*, 26(13), pp. 17066–17077, 2018. <https://doi.org/10.1364/OE.26.017066>
- [3] Mohammed, J. R. "Rectangular Grid Antennas with Various Boundary Square-Rings Array", *Progress In Electromagnetics Research Letters*, 96, pp. 27–36, 2021. <https://doi.org/10.2528/PIERL20112402>
- [4] Mohammed, J. R., Sayidmarie, K. H. "Sidelobe Cancellation for Uniformly Excited Planar Array Antennas by Controlling the Side Elements", *IEEE Antennas and Wireless Propagation Letters*, 13, pp. 987–990, 2014. <https://doi.org/10.1109/LAWP.2014.2325025>
- [5] Mohammed, J. R. "Synthesizing Sum and Difference Patterns with Low Complexity Feeding Network by Sharing Element Excitations", *International Journal of Antennas and Propagation*, 2017, 2563901, 2017. <https://doi.org/10.1155/2017/2563901>
- [6] Balanis, C. A. "Antenna Theory: Analysis and Design", Wiley, 2016. ISBN 978-1-118-64206-1
- [7] Skolnik, M. I. "Introduction to radar systems", McGraw Hill, 1980. ISBN 9780070579095
- [8] Comisso, M., Vescovo, R. "Multi-beam synthesis with null constraints by phase control for antenna arrays of arbitrary geometry", *Electronics Letters*, 43(7), pp. 374–375, 2007. <https://doi.org/10.1049/el:20070167>
- [9] Tsai, Y.-C., Chen, Y.-B., Hwang, R.-B. "Combining the switched-beam and beam-steering capabilities in a 2-D phased array antenna system", *Radio Science*, 51(1), pp. 47–58, 2016. <https://doi.org/10.1002/2015RS005764>
- [10] Sayidmarie, K., Mohammed, J. R. "Performance of a Wide Angle and Wideband Nulling Method for Phased Arrays", *Progress In Electromagnetics Research M*, 33, pp. 239–249, 2013. <https://doi.org/10.2528/PIERM13100603>
- [11] Sabaawi, A. M. A., Younus, K. M. "Multiband Handset Antenna System for UMTS/LTE/WLAN/Sub-6 5G and mmWave 5G Future Smartphones", *Periodica Polytechnica Electrical Engineering and Computer Science*, 66(2), pp. 116–121, 2022. <https://doi.org/10.3311/PPee.19679>
- [12] Mohammed, J. R. "Obtaining Wide Steered Nulls in Linear Array Patterns by Controlling the Locations of Two Edge Elements", *AEÜ - International Journal of Electronics and Communications*, 101, pp. 145–151, 2019. <https://doi.org/10.1016/j.aeue.2019.02.004>
- [13] Mohammed, J. R., Sayidmarie, K. H. "Performance Evaluation of the Adaptive Sidelobe Canceller with various Auxiliary Configurations", *AEÜ - International Journal of Electronics and Communications*, 80, pp. 179–185, 2017. <https://doi.org/10.1016/j.aeue.2017.06.039>

- [14] Mohammed, J. R. "A New Simple Adaptive Noise Cancellation Scheme Based On ALE and NLMS Filter", In: Fifth Annual Conference on Communication Networks and Service Research (CNSR '07), Fredericton, NB, Canada, 2007, pp. 245–254. ISBN 0-7695-2835-X  
<https://doi.org/10.1109/CNSR.2007.4>
- [15] Mohammed, J. R. "Optimal Null Steering Method in Uniformly Excited Equally Spaced Linear Array by Optimizing Two Edge Elements", *Electronics Letters*, 53(13), pp. 835–837, 2017.  
<https://doi.org/10.1049/el.2017.1405>